The Effects of Clouds on the Diurnal Variation of Underwater Irradiances on Horizontal Surfaces

JACK A. C. KAISER

Ocean Sciences Division, Naval Research Laboratory, Washington, DC 20375

22 May 1978 and 20 March 1979

ABSTRACT

Measurements of underwater downwelling D, underwater upwelling U, both at 5 m, and surface downwelling irradiance I were taken over most of a 5-day period in August and September 1974 south and west of Bermuda. On clear days D/I reached a pronounced maximum at local noon, whereas U/I had a weak minimum at midday. On cloudy days both of the above ratios were larger at all times of the day and did not exhibit the midday maximum.

An absorption model for D/I is constructed by decomposing I into components from the sun, clear sky and clouds. The major differences between the components is their spectral and radiance distributions. Atmospheric water vapor and sea surface roughness effects are included. The model agrees with the experimental values of D/I to within 5% of I for all the data, and it reproduces the variation of this ratio with solar zenith angle and cloud cover.

1. Introduction

Very few data are readily available concerning the diurnal variation of wide-band underwater downwelling and upwelling irradiance and the effects of the degree of cloudiness on these quantities. For heat balance studies, these data are vitally necessary since the divergences of these irradiances are the thermal forcing functions—collectively they represent the largest component of the heat balance (Kaiser, 1978). Most underwater irradiance measurements appear to have been done with either visibility or photosynthetic processes in mind. For these purposes, a narrow-band detector is used and measurements are made at one or a few solar zenith angles. Recently, however, Paulson and Simpson (1977) used a semi-wideband detector to obtain downwelling irradiance profiles under clear and overcast skies in the North Pacific for a few low solar elevations ($\leq 38°$).

During a 5-day period in August and September 1974 in the vicinity of Bermuda, nearly continuous underwater upwelling and downwelling irradiance measurements at a 5 m depth were made under sunny and partly cloudy skies. The sensors used had an essentially flat response from 0.3 to 3 μm and underwater their response was within 7% of the ideal cosine collector. The data show a definite diurnal variation under sunny skies and a marked effect due to clouds. A simple absorption model of underwater downwelling irradiance agrees with this behavior.

2. Measurement technique

Two Eppley 8-48 black and white pyranometers, one uplooking and one downlooking, were used because of their flat spectral response. They were mounted on a "sled" which was towed 100 m behind a ship at a depth of 5 m. Its depth and orientation with respect to the vertical were monitored continuously by a pressure transducer and two mutually orthogonal pendulum inclinometers. The sled was usually towed at 4 kt, but every 30 min the ship speed was reduced to 1 kt in order to take a set of readings. At 1 kt the collectors of the pyranometers were aligned within 3° of horizontal, and the depth of the sled was within 0.05 m of the desired 5 m. Further details concerning this configuration are given by Kaiser (1976). All quantities were continuously recorded on strip chart recorders.

The pyranometers have hemispheric glass domes covering a flat plate collector. The instruments are calibrated at the factory in air, but after immersion in water the domes act as a strongly divergent lens, reducing the irradiance falling on the collector by about 45%. This effect had been noted by Gordon and Brown (1972). To determine the immersion effects, a careful laboratory calibration was made using an incandescent lamp as a semi-collimated light source. Since the correction factor ultimately depends on the radiance distribution of the ambient light field (Kaiser, 1976), the calibrations were made as a function of angle with respect to the flat plate collector of the pyranometers. Using underwater radiance distributions representing a clear and an overcast sky as given by Tyler and Preisendorfer (1962) and an assumed distribution representing the sun at 60° from the zenith, correction factors for each of these cases were calculated and found to be within 1% of each other. Hence, one correction factor for each pyranometer could be used for all the data. The correction factors (the ratio of actual to measured irradiance) were 1.725 for the

Unauthenticated | Downloaded 11/28/23 04:51 PM UTC

downwelling and 1.578 for the upwelling pyranometer. The correction factor is highly dependent on the position of the flat collector relative to the hemispheric glass domes, and small variations in manufacture can cause large variations in the correction factor.

The angular response of each instrument was within 2% of a cosine curve for zenith angles ≤70° in air, and within 7% in the same range of zenith angles underwater.

The pyranometers used here are normally intended for irradiance levels much larger than seen by the downlooking instrument, and there is no *a priori* assurance they are linear down to 10 W m^{-2}. This was checked by subjecting the instruments to irradiances from 1 to 200 W m^{-2}, and at each of the several "background" irradiances used in this range constant increments in irradiance of 0.9 and 6 W m^{-2} were added to the background irradiance. This was done by use of two lamps; the incrementing lamp was switched on and off while the background lamp remained constant. For both uplooking and downlooking pyranometers, the slope of the calibration curve as determined by this method was constant to within 2%, which is the limit of the measurement accuracy.

Since the sled on which the pyranometers were mounted was towed 100 m behind the ship, the ship occluded a negligible portion (0.007 sr) of the field of view of the uplooking pyranometer. The sled was supported by a float assembly at the surface; this obscured 0.008 sr of the field. At most, 0.4% of the Snell circle was obscured at any one time by the combined effects.

3. Results

Measurements were made over portions of 5 days in conjunction with heat content measurements. On two of the days, measurements spanned the entire daylight period. The first of these (28 August 1974) was in the vicinity of 31.5°N, 64.8°W (50–80 km south of Bermuda), and the second day (7 September 74) was near 34.5°N, 72.0°W (~300 km east of the Virginia Capes). On 28 August it was predominantly cloudy with sky cover varying from 0.5 to 0.9; 7 September had a sky cover range of 0 to 0.3 except near sunset. During both days the sea was relatively quiet with 1 m swell and 0.3–0.7 m seas. In addition to the underwater upwelling and downwelling irradiance measurements, all at a depth of 5 ± 0.05 m, the downwelling irradiance I at 5 m above the sea surface was measured aboard ship with another Eppley 8-48 pyranometer. Fig. 1 shows the daily variations of I, D, U and cloud cover for these two contrasting days.

The cloudy day (7 September) had a total I of 19.58 MJ m^{-2} while the total for the near-clear day (28 August) was only 19.92 MJ m^{-2}; hence the total downwelling irradiance differed only by 1.7%

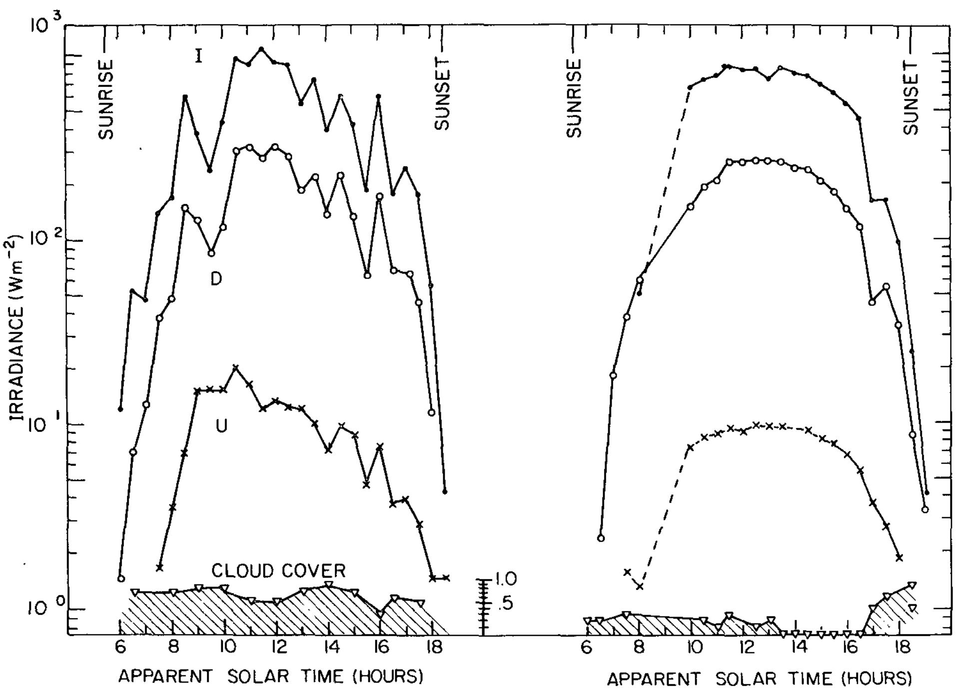

FIG. 1. Measured irradiances on a predominantly cloudy and a predominantly clear day. The surface downwelling irradiance is I and the underwater irradiances at 5 m are downwelling D and upwelling U.

Unauthenticated | Downloaded 11/28/23 04:51 PM UTC

although the average cloud covers C were 0.65 and 0.18, respectively. Daily irradiance totals were obtained by summing 15 min "eyeball" averages of the pyranometer records.

All the data were divided into two sets: for "clear" days when $C \leq 0.2$ and for "cloudy" days when $C \geq 0.2$. Two full days of measurements were classified as clear. For these days the ratios of D/I, U/D, and U/I are plotted in Fig. 2. I represents the irradiance incident upon the sea surface, and does not take account of the reflectivity of the sea surface. When the total cloud cover is 0.2 or less, D/I varies between 0.24 and 0.34 at a depth of 5 m; this ratio has its maximum just after apparent noon; data within 2 h of sunrise and sunset are uncertain because of the low levels of D and U. Hanson and Poindexter (1972) measured the irradiance transmittance of the upper 5 m of the ocean as a function of solar zenith angle and found that a quantity proportional to D/I showed a decrease with increasing zenith angles which is in qualitative agreement with the diurnal variation found here. U/D data were obtained by Ageronov (1964) and Jerlov (1968, p. 131) in the visible region, and they indicate a minimum approximately at apparent noon as shown in Fig. 2.

When the cloud cover is greater than 0.2 a more varied picture emerges. The irradiance ratios for clear or near-clear skies appear to set lower limits on those for cloudy days as Fig. 3 shows—the curves are for near-clear conditions, and all points are for conditions with cloud covers of 0.3 or more. Unlike the clear sky data, these data show no distinguishable diurnal trend. Tyler and Preisendorfer (1962) found in lake water that U/D is also greater under cloudy skies than under sunny skies.

Jerlov (1968) classifies water types optically by the percentage of total irradiance at various depths for a solar elevation of 90°. At a depth of 5 m, Jerlov's Type I oceanic water would have a downwelling irradiance of 0.3 I. For our measurements for 0.2 cloud cover or less, this ratio varied between 0.24 and 0.35, the larger value occurring when the sun was higher in the sky (21.3° zenith angle).

4. Comparison with a model

A purely absorption model of radiative transfer in the upper ocean (which can only predict D/I) was constructed to predict the downwelling irradiance as a function of depth, solar zenith angle and cloud cover. The effect of water vapor on the atmospheric absorption of incoming infrared radiation and the change in sea surface roughness with wind speed were included. Also, the radiance distribution of a clear sky was parameterized as a

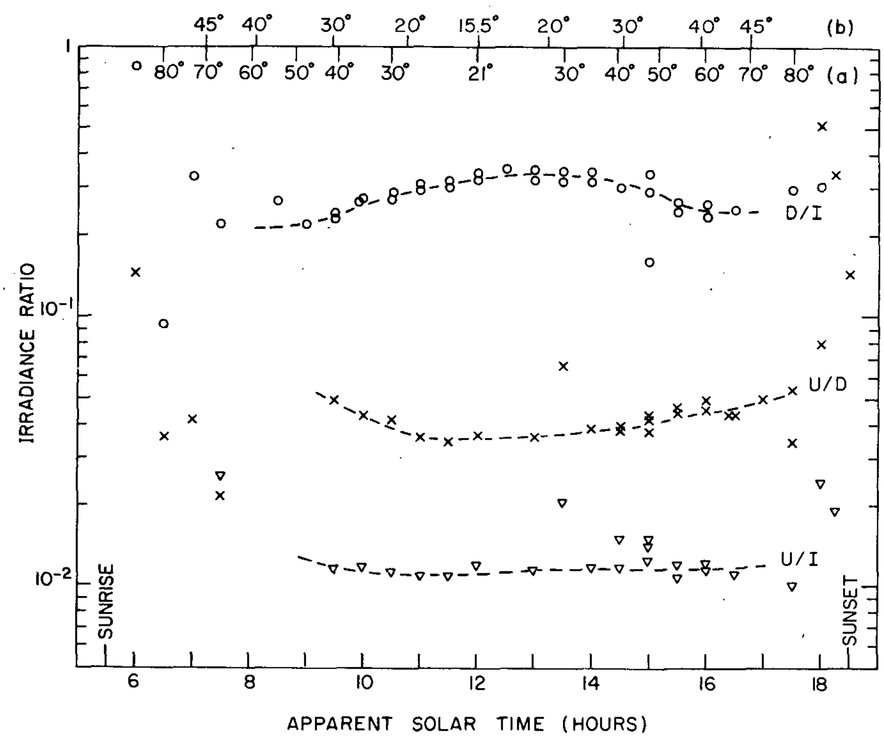

FIG. 2. Irradiance ratios on predominantly clear days ($C < 0.2$). The actual zenith angle of the sun (a) and the apparent underwater zenith angle due to refraction (b) are shown.

Unauthenticated | Downloaded 11/28/23 04:51 PM UTC

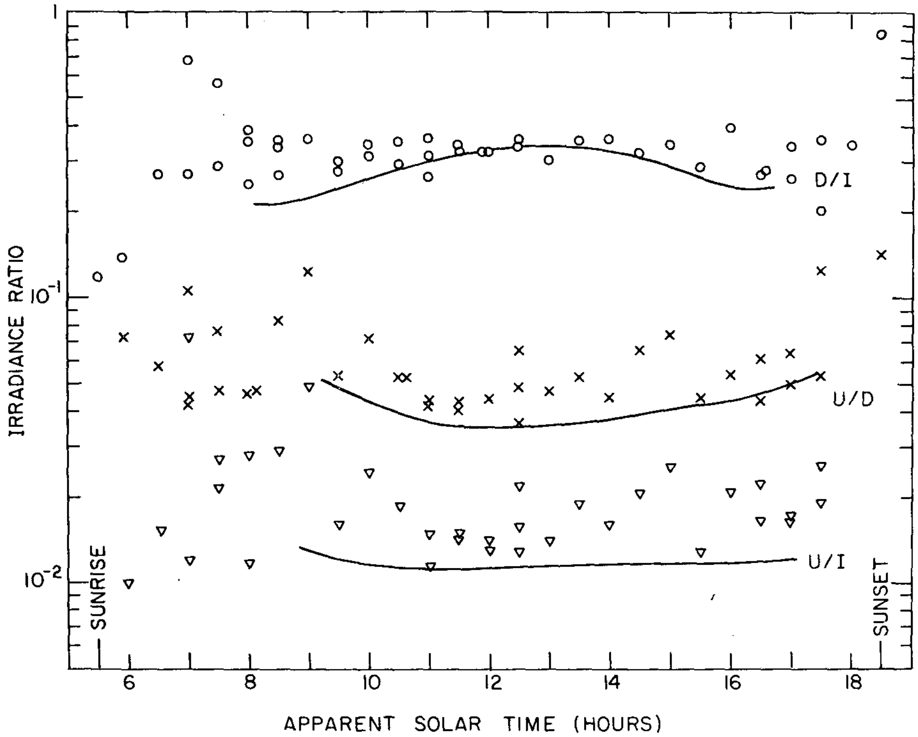

FIG. 3. Irradiance ratios (×'s) on predominantly cloudy days ($C \geq 0.3$) compared to those on predominantly clear days (curves).

first step to include atmospheric aerosols and dust. The model takes measured solar spectra at sea level as a function of air mass, calculated spectra for a pure Rayleigh sky, and cloud spectra determined from a two-flow model of radiative transfer in a model cloud having a liquid water content of 0.2 g m^{-3} and a thickness of 1.5 km. The direct solar radiation comes from a point source, but the sky and clouds are treated as distributed sources.

The three radiance fields are transmitted through the ruffled sea surface and then selectively absorbed by the water. The total spectrum is decomposed into 95 variable-width bins depending on the variability of the absorption coefficient and incoming intensity with wavelength. Details of this model are given in the Appendix.

From this model the ratio $\mathcal{R} = D/I$ at 5 m was calculated for one day in which the maximum solar elevation was 69° (to correspond to the measurements). The lowest curve of Fig. 4 is for a clear sky ($C = 0$), the intermediate one for scattered clouds ($C = 0.2$), and the top one for a solid overcast ($C = 1.0$). The clear to partly cloudy curves have maxima at noon for two reasons: 1) as the sun becomes highest in the sky, the radiation from it traverses the shortest path in the water; and 2) the reflectivity of the sea surface is smaller for a higher sun. As the sky becomes more cloudy, the portion of the irradiance field from the sun which traverses the sky becomes less prominent, so $\mathcal{R}$ varies much less with zenith angle.

As C increases, the spectral content of the irradiance changes. The clouds absorb more of the red of the direct solar beam so the total downwelling irradiance is much more bluish. Blue is not as highly absorbed as the red so $\mathcal{R}$ will increase as C increases.

In Fig. 4 the open circles represent measured values of $\mathcal{R}$ for $0 \leq C \leq 0.2$, and the solid circles, values of $\mathcal{R}$ for $0.2 \leq C \leq 1.0$. The shaded band is calculated from the model for $0 \leq C \leq 0.2$ and the open band for $0.2 \leq C \leq 1.0$. General agreement between the measurements and results of the model occurs in that the model predicts a maximum value of $\mathcal{R}$ at apparent noon for $C < 1.0$ and all values of $\mathcal{R}$ for $C > 0.2$ are larger than for $C < 0.2$. The overall range of values of $\mathcal{R}$ at 5 m is properly bracketed by the model.

The most likely source of disagreement between the model and the measurements is the ratio of the direct solar irradiance to the total irradiance Q, and its dependence on the solar zenith angle ψ—this certainly is highly variable under different atmospheric states, and concurrent measurements of this ratio would be useful. Values of $Q(\psi)$ were taken from List (1958) and Robinson (1962). Of course, the standard spectral distributions also may not be representative, and to refine the model, these should be reevaluated. The exclusion of

Unauthenticated | Downloaded 11/28/23 04:51 PM UTC

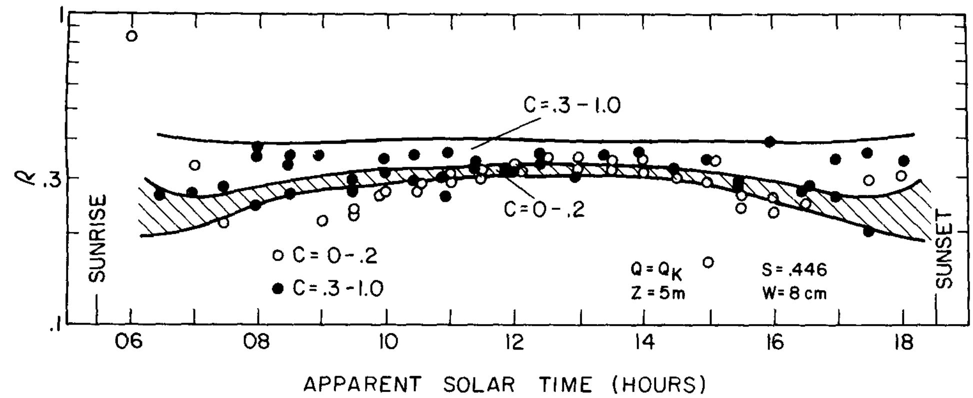

FIG. 4. A comparison of results from the irradiance model with measurements at 5 m depth. The open circles are for $C \leq 0.2$, and the solid circles for $C \geq 0.3$. The shaded zone is the model prediction for $0 \leq C \leq 0.2$, and the open zone for $0.2 \leq C \leq 1.0$. The ratio $\mathscr{R} = D/I$. The model predicts the maximum in $\mathscr{R}$ for $C \leq 0.2$ at local noon and that $\mathscr{R}(C \geq 0.3) > \mathscr{R}(C \leq 0.2)$; model values generally bracket the observed $\mathscr{R}$ values.

scattering in the water is thought not to be serious for calculations of D in the Sargasso Sea.

Acknowledgments. The author wishes to thank the crew of the USNS *Lynch* for their cooperation, and Robert Hill of the Naval Research Laboratory for providing the surface pyranometer data.

APPENDIX

Underwater Downwelling Irradiance Absorption Model

The downwelling irradiance is decomposed according to source: that directly from the sun, the sky and the clouds. The sky radiation is further split into a portion which transits with the sun, and the rest which is stationary with changing solar zenith angle. The radiation is partially reflected (or transmitted) at the sea surface, and the transmittances depend on the radiation source and the wind speed. After passing through the air-sea interface, the radiation is absorbed in the water. This absorption is a function of the spectral composition of the radiation and the radiance distribution of the source. Here scattering in the water is ignored, so the results necessarily apply to very clear waters such as the Sargasso Sea and of course only predict D.

At any time, only two sky conditions can occur:

1) When the sun is not obscured and downwelling irradiance above the surface is

$$A_1 = A_0 + A_d(1 - C) + CA_c, \qquad \text{(A1)}$$

where A_0 is the irradiance directly from the sun, C the cloud cover $(0 \leq C \leq 1)$, A_d the diffuse component of downwelling irradiance which would occur with a clear sky and A_c the total downwelling irradiance from a totally overcast sky if the clouds had the same brightness as they actually do for a partly cloudy sky. Actually A_d and A_c are almost the same but they do result from different radiance distributions. It is tacitly assumed that the clouds are randomly distributed in the sky at any time.

2) The other sky condition is when the sun is obscured. In this case the downwelling irradiance is

$$A_2 = A_d(1 - C) + CA_c. \qquad \text{(A2)}$$

If we assume C also represents the fraction of time a cloud obscures the sun, the time-average downwelling irradiance above the sea is

$$A_+ = A_1(1 - C) + A_2C \qquad \text{(A3)}$$

or, from (1) and (2),

$$A_+ = (A_0 + A_d)(1 - C) + A_cC. \qquad \text{(A4)}$$

Just below the sea surface

$$A_- = (\tau_0 A_0 + \tau_d A_d)(1 - C) + \tau_c A_c C, \qquad \text{(A5)}$$

where τ_0, τ_d and τ_c are surface transmittances for the three components of radiation. The values are given in Cox and Munk (1956) for wind speeds of 0 and 7 m s^{-1}.

At any given depth z, each component of irradiance is attenuated by absorption and

$$A_-(z) = (\tau_0 I_0 A_0 + \tau_d I_d A_d)(1 - C) + \tau_c I_c A_c C, \qquad \text{(A6)}$$

where I_0 is the ratio of the direct beam irradiance at depth z to the direct beam irradiance just below the sea surface, and I_d and I_C are the similar ratios for the sky and cloud irradiances, i.e., they represent the transmittancy of the ocean from the surface to z for each source. The quantities A_0, A_d and A_c need to be related to direct observables, in this case, the solar zenith angle ψ, the cloud cover C, and the ratio Q of the irradiance due to the direct com-

Unauthenticated | Downloaded 11/28/23 04:51 PM UTC

ponent of radiation to the total clear-sky irradiance. Thus we have

$$Q = A_0/(A_0 + A_d). \quad \text{(A7)}$$

Values of Q can be obtained from List (1958) or Robinson (1962). From Kaiser and Hill (1976),

$$A_+ = (A_0 + A_d)(1 - 0.55C^{1.75}). \quad \text{(A8)}$$

Combining (8) with (4) yields

$$A_c = (A_0 + A_d)(1 - 0.55\, C^{0.75}) \quad \text{(A9)}$$

and the ratio $\mathscr{R} = A_-(z)/A_+$ is

$$\mathscr{R} = \frac{(1 - C)[\tau_0 Q I_0 + \tau_0(1 - Q)I_d] + \tau_c I_c(1 - 0.55C^{0.75})C}{(1 - 0.55C^{1.75})}. \quad \text{(A10)}$$

The ratio $\mathscr{R}$ at 5 m is the same as D/I.

The diffuse component can further be divided into a portion S which is stationary with respect to ψ and a remainder $(1 - S)$ which moves with the sun. Values of S were obtained from the sky radiance distributions of Hopkinson (1954). In this case the sky term becomes

$$\tau_d I_d \rightarrow \tau_d S I_d + \tau_0 I_d(1 - S), \quad (11)$$

so, finally,

$$\mathscr{R} = \frac{(1 - C)\{\tau_0 I_0 Q + [\tau_d I_d S + \tau_0 I_d(1 - S)](1 - Q)\} + \tau_c I_c C(1 - 0.55C^{0.75})}{(1 - 0.55C^{1.75})}. \quad (12)$$

The I's were determined from

$$I = \int I_\lambda \exp(-\alpha_\lambda \gamma z) d\lambda \Big/ \int I_\lambda d\lambda. \quad (13)$$

The $I_{0,\lambda}$ spectra at 0 km are taken from Kondratyev (1973); the $I_{d,\lambda}$ spectra from Deirmendjian and Sekera (1954) (a pure Rayleigh sky); and the $I_{c,\lambda}$ spectra are obtained by taking $I_{0,\lambda}$ at 3 km from Kondratyev (1973) and passing it through a radiative transfer model for a cloud due to Middleton (1954). The cloud has 0.2 g m^{-3} liquid water and is 1.5 km thick. The absorption coefficients d_λ are from Irvine and Pollack (1968). γ represents an effective path factor. For the sun and transitory sky radiation $\gamma = \sec\psi'$, where ψ' is the underwater solar zenith angle. For the sky $\gamma = 1.25$ and for clouds, $\gamma = 1.17$; these two path factors represent weighted penetration depth factors due to the diffuse nature of the source. z is the depth in meters.

To account for atmospheric water vapor content, the factor $\exp w^{1/2}$ was used in the water absorption bands (Gates, 1966); w is the liquid water content of the clouds in precipitable centimeters.

REFERENCES

Ageronov, V. K., 1964. On the daily fluctuations of radiant energy of the sun in the layers of the ocean in relation to its optical density. *Tr. Morsk. Gidrofiz. Issled. Akad. Nauk. SSSR*, **29**, 76–83.

Cox, C., and W. Munk, 1956: Slopes of the sea surface deduced from photographs of sun glitter. *Bull. Scripps Inst. Oceanogr.*, **6**, 401–488.

Deirmendjian, D., and Z. Sekera, 1954: Global radiation resulting from multiple scattering in a Rayleigh atmosphere. *Tellus*, **6**, 382–398.

Gates, D. M., 1966: Spectral distribution of solar radiation at the earth's surface. *Science*, **151**, 523–529.

Gordon, H. R., and O. B. Brown, 1972: Immersion corrections for the Eppley underwater pyranometer. *Preprints Conf. Atmospheric Radiation*, Fort Collins, Amer. Meteor. Soc., 163–164.

Hanson, K. J., and M. F. Poindexter, 1972: Attenuance of broad-band solar irradiation in the ocean. *Preprints Conf. Atmospheric Radiation*, Fort Collins, Amer. Meteor. Soc., 165–168.

Hopkinson, R. G., 1954: Measurements of sky luminance distribution at Stockholm. *J. Opt. Soc. Amer.*, **44**, 455–459.

Irvine, W., and J. Pollack, 1968: Infrared optical properties of water and ice spheres. *Icarus*, **8**, 324–360.

Jerlov, N. G., 1968: *Optical Oceanography*. Elsevier.

Kaiser, J. A. C., 1976: The use of pyranometers for underwater total radiant energy flux measurement. *Deep-Sea Res.*, **23**, 881–887.

——, 1978: Heat balance of the upper ocean under light winds. *J. Phys. Oceanogr.*, **8**, 1–12.

——, and R. H. Hill, 1976. The influence of small cloud covers on the global irradiance at sea. *J. Geophys. Res.*, **81**, 395–398.

Kondratyev, K., 1973: *Radiation Characteristics of the Atmosphere*. NASA TT F-678, Amerind Publ. Co., New Delhi.

List, N., Ed., 1958: *Smithsonian Meteorological Tables*, 6th ed. Smithsonian Institute, Washington, DC, 439 pp.

Middleton, W. E. K., 1954: The color of the overcast sky. *J. Opt. Soc. Amer.*, **44**, 793–798.

Paulson, C. A., and J. J. Simpson, 1977: Irradiance measurements in the upper ocean. *J. Phys. Oceanogr.*, **8**, 952–956.

Robinson, G. D., 1962: Absorption of solar radiation by atmospheric aerosol, as revealed by measurements at the ground. *Arch. Meteor. Geophys. Bioklim.*, **B12**, 19–40.

Tyler, J. E., and R. W. Preisendorfer, 1962: Transmission of energy within the sea: Light. *The Sea*, M. N. Hill, Ed., Vol. 1. Interscience, 397–451.

Unauthenticated | Downloaded 11/28/23 04:51 PM UTC